Two-level model of longitudinal magnetic field-induced current instability and chaos in *n*-GaAs

Shwu-Yun Tsay Tzeng[1,*] and Yiharn Tzeng[2]
[1]*Department of Electro-Optical Engineering, National Taipei University of Technology, Taipei, Taiwan 106, Republic of China*
[2]*Institute of Physics, Academia Sinica, Taipei, Taiwan 115, Republic of China*
(Received 8 August 2005; published 8 November 2005)

We extend our previous application of the two-impurity-level model to interpret the cross-over current instability for a *n*-GaAs semiconductor with planar ohmic contacts under an external magnetic field *B* longitudinal to the applied dc bias. The previous assumption of spatial homogeneity in current flow direction as well as previous considerations of the Landau level shifts for the conduction band electrons and the electron mobility with the field and the carrier electron temperature dependence are all retained. In addition, we further add in a phenomenological effective magnetoresistance *h* factor from the generation-annihilation dynamic of the filamentary current and the carrier temperature dependence of the impact ionization coefficient from the ground level X_1 and that of the capture coefficient T_1^s in the generation-recombination processes. Increasing the magnetic field above a critical magnitude in the post-breakdown region of the S-shaped current density-field characteristic, we are able to find the system bifurcating to chaos via several period-doubling routes at various bias voltages. Our numerical results are consistent with those observed experimentally by Aoki, Kawase, Yamamoto, and Mugibayahi [J. Phys. Soc. Jpn. **59**, 20 (1990)].

DOI: 10.1103/PhysRevB.72.205201 PACS number(s): 72.20.Ht

I. INTRODUCTION

Semiconductors with S-shaped current density-field characteristics and negative differential conductivity (SNDC) under dc bias voltages are rich in many interesting nonlinear characteristics. Examples among those already discovered include the hysteresis of the static current-voltage,[1–3] breathing filaments,[4–11] self-sustained chaotic current or voltage oscillation,[3,12–18] and so on. Many of the above nonlinear transport properties can be described by the well-established two-impurity-level model.[3]

A number of experimental works have been reported on these behaviors associated with the impact ionization processes of neutral shallow impurities in many bulk semiconductor materials, under various experimental conditions such as different orientations of applied magnetic fields.[1,2,19] The hysteresis of *I-V* curve for a *n*-GaAs semiconductor subject to an external magnetic field *B* longitudinal or transverse to the applied dc bias has been investigated by Aoki *et al.*[1,2] and Aoki and Kondo.[20] In addition, they also found that for the longitudinal *B* case, the hysteresis fades away as *B* increases beyond a certain magnitude, and the spontaneous cross-over instability occurs as *B* is further lifted above a critical value B_c.

The above-mentioned hysteresis phenomena from the system under both orientations of the magnetic field *B* were nicely interpreted in our previous work,[21] where we adopted a two-impurity-level model, with the assumptions of spatial homogeneity in current flow for the planar-type ohmic contacts[6] and instantaneous energy balance, along with a careful treatment on the magnetoresistance property. In an earlier publication,[22] the two-level model was also successfully applied to describe experimentally observed limit cycle oscillations, bifurcations, or chaos in dynamic Hall effects, when a transverse magnetic field is imposed to *n*-GaAs at helium temperatures.[19] In this paper we would like to extend our model to explain the characteristics of the current instabilities observed in Refs. 1 and 2 under the longitudinal *B* fields. After doing so we will thus be able to reproduce theoretically the phenomena of hysteresis and the current instabilities for systems under either a transverse or a longitudinal *B* by the two-level model consistently.

In the two-level model, the electronic states of a donor impurity consist of the ground and the first excited levels. The carrier density *n* in the conduction band is determined by the generation-recombination (GR) processes in which an electron in these impurity states may be thermally ionized or impact ionized to the conduction band, and may then recombine with a donor having an empty state. The definitions of the GR coefficients X_1^s, T_1^s, X_1, X_1^*, X^*, and T^* can be found in Fig. 1 in Ref. 21 or Ref. 22.

In our previous work,[21] we have discussed in details the influence of the applied external magnetic field on the GR processes, especially the thermal ionization and the impact ionization, through several aspects, such as Landau level shifts for the electrons in the conduction band, the magnetoresistance, and the modification on the cross sections of the impact ionization. These effects are indeed important in our previous analysis of hysteresis phenomena and will also be retained in this work.

These GR coefficients depend not only on the electric field *E*, but also on the electron concentration *n*. From *E* and *n*, there are several ways to determine the electron temperature T_e, for example, fitting to the Monte Carlo simulation,[23] and calculating from the energy balance equation.[24] To be consistent with our previous works[21,22] here we also extract T_e from the energy balance equation. We have already considered some of these GR coefficients' T_e dependence implicitly or explicitly in Ref. 21. The cross-over instability occurs in the post-breakdown region. Around this region, the obvious variations of T_e, the impact ionization coefficient from the ground level X_1, and the capture coefficient T_1^s with *E* were demonstrated in studies with Monte Carlo simulations.[23,25] This implies that the T_e dependence of these

GR coefficients should be taken into account more seriously. We thus add in the T_e dependence of T_1^s and modify our previous X_1. Indeed we find the T_e dependence an important ingredient in this work to interpret the cross-over instability. This T_e dependence along with the detailed description of our model will be discussed in the next section.

We then apply the extensive two-impurity-level model to the post-breakdown region of the S-shaped current density-field characteristic for a n-GaAs semiconductor under an external B longitudinal to the applied E. In this region, the filamentary current and the phenomena of cross-over instability and chaos were observed and described in detail in Refs. 1 and 2. To account for the effects from the current filament, a phenomenological magnetoresistance factor was suggested by Aoki.[24,26] We also adopt this magnetoresistance factor as it forms another indispensable constituent for our purpose in this work. Note that although here we are examining what were observed in Refs. 1 and 2 where experiments were set up with the planar-type ohmic contacts rather than those with point contacts,[27] we are certainly not in the position to judge the superiority or inferiority of any experiments. Results from our numerical simulations indicate that with a specified B larger than a critical B_c and a proper load condition, increasing the applied electric field can result in the system's undergoing a series of period-doubling routes to chaos. Our numerical results which will be presented in Sec. III, are consistent with those observed experimentally in Refs. 1 and 2.

II. MODEL

Let us start from the GR rate equations in the two-impurity-level model for a n-GaAs. In this model, the ground level density n_{t_1}, the first excited level density n_{t_2}, and the electron density n in the conduction band, satisfy the dynamical equations[3,13]

$$\dot{\nu} = X_1 N_D^* \nu \nu_{t_1} + (X_1^s + X_1^* N_D^* \nu)\nu_{t_2} - T_1^s N_D^* (N_A/N_D^* + \nu)\nu, \tag{1}$$

$$\dot{\nu}_{t_1} = -(X^* + X_1 N_D^* \nu)\nu_{t_1} + T^* \nu_{t_2}, \tag{2}$$

with $\nu = n/N_D^*$, …, etc., $N_D^* = N_D - N_A$ being the effective doping concentration, N_D, N_A the donor and the acceptor concentrations respectively, $\nu_{t_2} = 1 - \nu - \nu_{t_1}$ from the conservation of charge, and dot denoting the time derivative. The magnitudes of the GR coefficients at 4.2 K, the liquid-helium temperature, are given in Table I. As we will discuss in a moment, these coefficients may vary with various factors, such as changes of the electron temperature T_e, applications of external electric or magnetic fields, and so on.

Here we consider the case that a static electric field is applied in the x direction, $\mathbf{E_0} = E_0\hat{\mathbf{x}}$ and so is an external static magnetic field $\mathbf{B} = B\hat{\mathbf{x}}$. The dynamical equation for the drift electric field $\mathbf{E} = E\hat{\mathbf{x}}$ can be written as

$$\dot{E} = -\gamma_d\left(-E_0 + E + \frac{AR}{L}J\right) \tag{3}$$

with the current density

TABLE I. Parameters corresponding to n-GaAs at 4.2 K for the two-level GR mechanism.

Parameter	Value
T^*	10^6 s^{-1}
X_1^s	2×10^5 s^{-1}
X^*	3×10^5 s^{-1}
X_1^0	5×10^{-8} cm^3 s^{-1}
X_1^{*0}	10^{-6} cm^3 s^{-1}
e_1	9.58×10^{-8} cm^3 s^{-1}
g_1	1.16×10^{-6} cm^3 s^{-1}
(e_2, e_3)	(2.3, −0.095)
(g_2, g_3)	(−0.265, 1.254)
$(\nu_{\rm th}, q_1)$	(0.07, 0.693)
N_A/N_D^*	0.3
ϵ	$10\epsilon_0$
m^*	$0.066m_0$
μ_0	2.5×10^4 cm^2/V s
T_M	2.15
ν_c	1.87×10^{-2}
α	4.82×10^2
T_L	4.2 K
β_0^2	3×10^2
ν_0	5.75×10^{-3}
N_D^*	10^{15} cm^{-3}

$$J = e\nu N_D^* \mu_B E, \tag{4}$$

where $1/\gamma_d$ is the effective dielectric relaxation time, μ_B the mobility in the magnetic field, R the load resistance, and L and A are, respectively, the length and the cross-sectional area of the sample.

During the GR processes the electron temperature T_e will increase and can be determined through $\mathcal{E} = \frac{3}{2}k_B T_e$, with k_B being the Boltzmann constant. $\mathcal{E}$ is directly related to the electric field E via the energy balance equation[24]

$$\dot{\mathcal{E}} = -(\mathcal{E} - \mathcal{E}_L)/\tau(\mathcal{E}) + e\mu_B E^2 \tag{5}$$

where $\mathcal{E}_L = \frac{3}{2}k_B T_L$ is the thermal energy at zero-electric field with the lattice temperature T_L, and $\tau(\mathcal{E}) \propto \mathcal{E}^{-1/2}$ the energy relaxation time considered theoretically. In line with our previous work,[21] Eq. (5) is also converted to[28]

$$\dot{\bar{T}}_e = -\frac{1}{\tau_0}[\bar{T}_e^{\,1/2}(\bar{T}_e - 1)] + \frac{2e}{3k_B T_L}\mu_B E^2 \tag{6}$$

with $\bar{T}_e = T_e/T_L$ and τ_0 the energy relaxation time constant.

The mobility in the magnetic field μ_B appearing in Eqs. (4)–(6) is affected directly by the external magnetic field. With the help of the effective magnetoresistance factor h, one may write[24,26]

$$\mu_B = h\mu_{\rm BH}, \tag{7}$$

with $\mu_{\rm BH}$ being the carrier mobility in the zero-magnetic field. The factor h has different characteristics for different

orientations of the applied magnetic field. As for our case, when a longitudinal magnetic field B is applied, the current filament nucleated between two parallel ohmic contacts has been found from experiments.[29–33] The current flows are observed to be curved along the filament boundaries,[31–33] along where the current flows are not completely parallel to the field B and hence may experience a Lorentz force. This gives rise to the inhomogeneous magnetoresistance induced at the filament boundaries.

In a one-level model,[24] in order to explain the observed cross-over instability in n-GaAs, a simple relaxation-type equation is introduced phenomenologically for the h factor from the generation-annihilation dynamic of the filamentary current

$$\dot{h} = -\gamma(h - h_s), \tag{8}$$

with γ being a damping constant, and the static factor h_s as[24,26]

$$h_s = 1 - \frac{1}{2}T_M(\mu_0 B)^2\{1 + \tanh[\alpha(\nu - \nu_c)]\}. \tag{9}$$

In the above, T_M is the magnetoresistance scattering factor, μ_0 the zero-electric-field mobility at temperature T_L, α the inhomogeneity factor of the current filament, and ν_c is related to the critical density necessary for the current filamentation. The factor h_s is so chosen due to its different properties observed experimentally in different regimes in the current-voltage characteristic of the sample n-GaAs.[34]

In Eq. (7), the zero-magnetic-field mobility μ_{BH} of the electrons with density n at temperature T_e is given by Brooks-Herring (BH) (Ref. 35) as

$$\mu_{\mathrm{BH}} = \mu_0\left(\frac{T_e}{T_L}\right)^{3/2}\frac{2N_A/N_D^* + \nu_0}{2N_A/N_D^* + \nu}\frac{\ln(1+\beta_0^2) - \beta_0^2/(1+\beta_0^2)}{\ln(1+\beta^2) - \beta^2/(1+\beta^2)}, \tag{10}$$

with

$$\beta^2 = \beta_0^2\left(\frac{T_e}{T_L}\right)^2\frac{\nu}{\nu_0}, \tag{11}$$

where $\nu_0 = n_0/N_D^*$, and n_0 and β_0 are the electron density and the so-called BH coefficient, respectively, under the zero electric field at T_L, and $\nu = n/N_D^*$, n, β for those at temperature T_e. Since T_e can be determined from the energy balance equation Eqs. (5) and (6) and ν is related to the electric field by GR rate Eqs. (1) and (2), our μ_{BH} is dependent of the electron temperature and the electric field.

We will examine the cross-over instability for n-type GaAs by solving the coupled differential Eqs. (1)–(3), (6), and (8) with the considerations of the inhomogeneous magnetoresistance in Eqs. (7) and (9), as well as effects from the electric field E, magnetic field B, and the carrier temperature T_e variation. Besides explicitly appearing in the differential equations, these effects may also implicitly be embedded in the GR coefficients. We now take a look at this.

In our previous works,[21,22] we have added the magnetic field effects to the electric field and binding energy dependent Lucky electron model,[36] and write the impact-ionization coefficients X_1 and X_1^* as

$$X_1(E,B) = \alpha(B)X_1^0 e^{-\varepsilon_b^B h^{-1/2}/E}, \tag{12}$$

$$X_1^*(E,B) = \alpha^*(B)X_1^{*0} e^{-\varepsilon_b^{*B} h^{-1/2}/E}, \tag{13}$$

with coefficients X_1^0, X_1^{*0} being given in Table I. The magnetic field-dependent binding energies ε_b^B and ε_b^{*B} are defined as

$$\varepsilon_b^B = \varepsilon_b + \Delta\varepsilon_B, \tag{14}$$

$$\varepsilon_b^{*B} = \varepsilon_b^* + \Delta\varepsilon_B, \tag{15}$$

with $\varepsilon_b = 6.0$ meV and $\varepsilon_b^* = 1.5$ meV, the impurity ground and first excited state binding energies for n-GaAs, $\Delta\varepsilon_B = \hbar\omega_c^*/2$, $(\omega_c^* = eB/m^*c)$ the Landau level shift of conduction electrons, and $m^* = 0.066m_0$.

As suggested in Refs. 14, 24, and 37, the cross sections of the impact ionization are proportional to $\varepsilon_i^{1/2}(1+\gamma_0\mu\sqrt{\varepsilon_i})$, with ε_i the electron binding energy and γ_0 a constant. Hence in Eqs. (12) and (13), we have the cross sections of X_1^0 and X_1^{*0} multiplied by $\alpha(B)$ and $\alpha^*(B)$, respectively, with the forms

$$\alpha(B) = \left(\frac{\varepsilon_b^B}{\varepsilon_b}\right)^{1/2}\frac{1 + \eta h\sqrt{\varepsilon_b^B}}{1 + \eta\sqrt{\varepsilon_b}}, \tag{16}$$

$$\alpha^*(B) = \left(\frac{\varepsilon_b^{*B}}{\varepsilon_b^*}\right)^{1/2}\frac{1 + \eta h\sqrt{\varepsilon_b^{*B}}}{1 + \eta\sqrt{\varepsilon_b^*}}, \tag{17}$$

and constant $\eta = 0.4$. These two factors are exactly equal to 1 as $B = 0$.

For E higher than the breakdown field, X_1 and X_1^* behave differently toward T_e.[23,25] Because the excited state's ionization energy is much smaller than the ground state's, X_1^* shows a very weak dependence on T_e.[25]

However, things are different for X_1. Both T_e and X_1 show similar behaviors as E varies.[25] Hence we multiply a factor $\delta(T_e)$ to the cross section of X_1 as the temperature increases

$$\delta(T_e) = 1 + \lambda T_e/T_L, \tag{18}$$

where λ is an adjustable parameter and is taken to be 0.06. Thus $X_1(E,B)$ in Eq. (12) now reads

$$X_1(E,B,T_e) = \delta(T_e)\alpha(B)X_1^0 e^{-\varepsilon_b^B h^{-1/2}/E}, \tag{19}$$

while $X_1^*(E,B)$ retains the same form as that in Eq. (13).

In our previous work,[21] we have already taken into account the effects of the magnetic field and the temperature variation on the thermal ionization coefficients. Here we keep the same treatment and have the thermal ionization coefficient modified as

$$X_1^s(T_e,B) = X_1^s(T_L)e^{\varepsilon_b^*(1/k_BT_L - 1/k_BT_e)}e^{-\Delta\varepsilon_B/k_BT_e}. \tag{20}$$

As for the capture coefficient T_1^s, we adopt T_1^s from Ref. 23 as

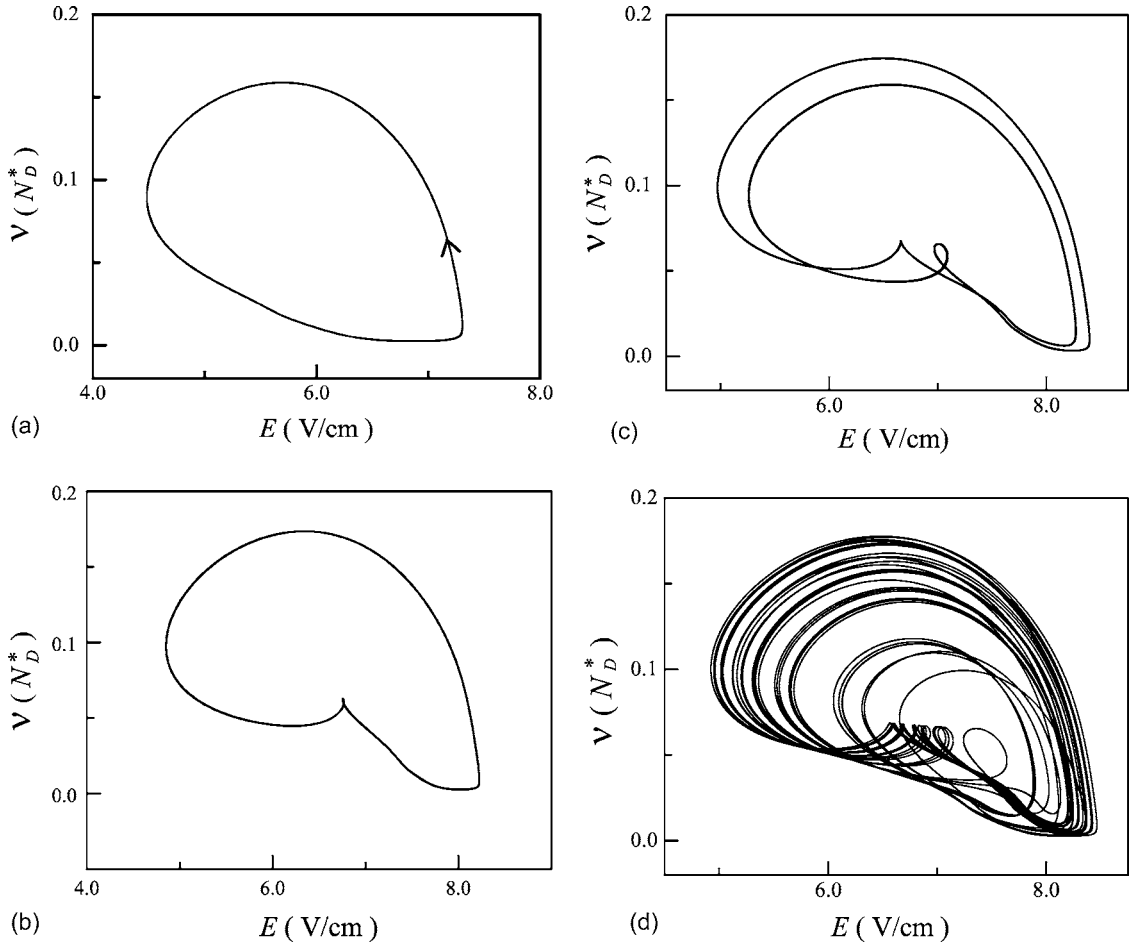

FIG. 1. Phase portraits of the conduction electron concentration ν versus the electric field E for the following control parameters E_0: (a) 7.72 V/cm, (b) 8.50 V/cm, (c) 8.70 V/cm, and (d) 8.75 V/cm.

$$T_1^s(T_e,\nu)=\frac{1}{2}\{[T_1^{s,\mathrm{up}}(T_e)+T_1^{s,\mathrm{lo}}(T_e)]+[T_1^{s,\mathrm{up}}(T_e)-T_1^{s,\mathrm{lo}}(T_e)]\tanh[\log_{10}(\nu/\nu_{\mathrm{th}})]\},$$

$$T_1^{s,\mathrm{up}}(T_e)=e_1\exp[e_2(T_e/T_L-q_1)^{e_3}],$$

$$T_1^{s,\mathrm{lo}}(T_e)=g_1\exp[g_2(T_e/T_L)^{g_3}], \tag{21}$$

with parameters ν_{th}, q_1, e_i, g_i, $i=1,\ldots,3$, being defined in Ref. 23. Here T_1^s is enhanced by the T_e dependent functions $T_1^{s,\mathrm{up}}(T_e)$ and $T_1^{s,\mathrm{lo}}(T_e)$ at the onset of the upper branch of the $n(E)$ characteristic due to strong impact ionization, from which many carriers are scattered back to the band minimum with high recombination probabilities.

III. SIMULATIONS AND NUMERICAL RESULTS

Earlier in Ref. 21, based on the two-impurity-level model, we satisfactorily described the experimentally observed hysteresis I-V characteristics for n-type semiconductors under both longitudinal and transverse B fields by putting differential Eqs. (1)–(3), (6), and (8) into steady conditions. Let us concentrate on the longitudinal B field case. Increasing B beyond a certain magnitude, we can see that the holding voltage of the hysteresis exceeds the breakdown voltage such that the hysteresis disappears. As B rises above a critical B_c, spontaneous oscillations start near the unstable state $(\nu,\nu_{t_1},E,h,\bar{T}_e)$. We now proceed to investigate the cross-over current instability by solving these differential equations with the considerations of the inhomogeneous magnetoresistance as well as the magnetic field and temperature dependent GR coefficients mentioned in the previous section.

Phenomenologically, the generation-annihilation process of the current filament is counted as an important factor to describe the cross-over instability.[24] During each period of the current oscillation, the local magnetoresistance may evolve cooperatively with the size evolution of the current filament. Therefore, the period of the spontaneous current oscillation is of the order or larger than the dielectric relaxation time. In our model simulation, the recombination time $1/\gamma$ in Eq. (8) is taken to be 2μs, which is longer than the effective dielectric relaxation time of the longitudinal electric field $1/\gamma_d$ ($\approx 1\mu$s).

The energy relaxation time τ_0 taken to be 6.79×10^{-11} s is considered theoretically much shorter than the effective dielectric-field relaxation time. Since the dynamics of the system is dominated by the slow process,[3] the effective di-

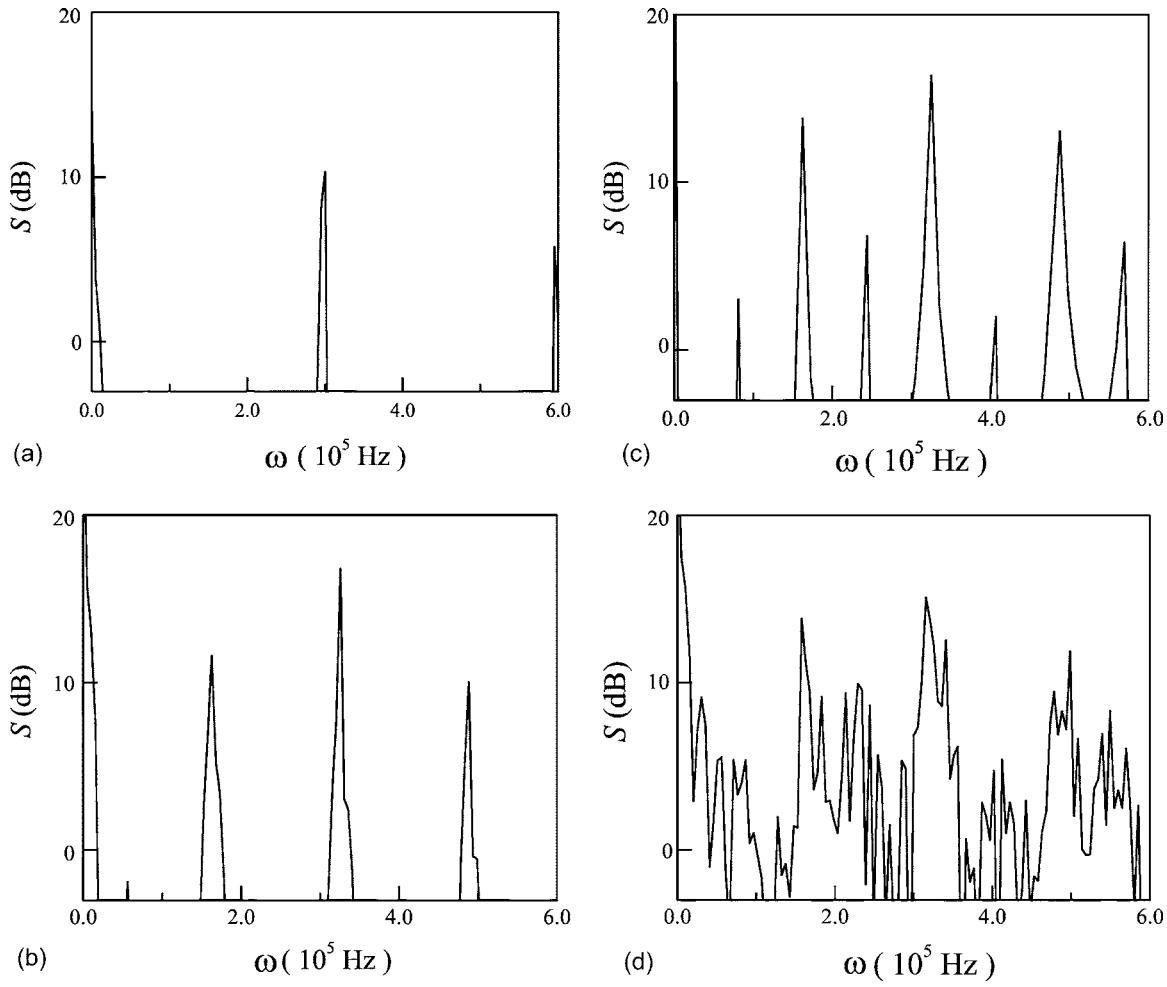

FIG. 2. Power spectra $S(\omega)$ of $\nu(t)$ corresponding to Figs. 1(a)–1(d), respectively.

electric relaxation time and the recombination time become important elements to determine the oscillation frequency.

In our numerical simulation, we set the applied electric field E_0 as the control parameter, and the longitudinal magnetic field B as an adjustable parameter. By setting the inclined load line $E_0=E+dJ$ in the post-breakdown region, we are able to solve the above-mentioned differential equations in a standard way at a specified B with the fixed load-line condition $d=AR/L$. We then obtain solutions from numerical procedures detailed in Ref. 22. The system can be seen to undergo a series of period-doubling routes to chaos as the control parameter E_0 increases.

Setting the load-line condition at $d=5.32$ cm VA^{-1} in our computation, and increasing gradually the magnitude of B beyond the disappearance of the hysteresis, we can see period-1 and period-2 oscillations at $B=165$ mT with proper E_0 values. As B goes on increasing to around 180 mT oscillations up to period 4 can be seen, and at $B=185$ mT chaos comes in. Note that E_0 varies with B for a certain oscillation's or chaos' appearing.

Examples of our numerical results with the magnetic field being fixed at $B=200$ mT are shown in Figs. 1 and 2. Figures 1(a)–1(d) present the projection of the phase portrait in the (ν,E) plane for period 1, period 2, period 4, and chaos as the control parameter E_0 set to be 7.72, 8.50, 8.70, and 8.75 V/cm, respectively. Here besides a limit cycle oscillation, we have also found period-two, period-four, and period-eight oscillations, but as E_0 increases further beyond the critical field the oscillations become nonperiodic and random which indicates a sign of chaos.

The corresponding Fourier power spectra of $\nu(t)$ are shown in Figs. 2(a)–2(d) where we see that the natural frequency of the spontaneous electron density oscillations is in the order of 10^5 Hz, the same order as the frequency given by the recombination time $1/\gamma$, and the effective dielectric relaxation time $1/\gamma_d$ of the longitudinal electric field. The results indicate that the period doubling bifurcations can clearly be seen in the post-breakdown regime by increasing the voltage bias from 7.72 to 8.75 V/cm.

IV. CONCLUSION

In summary, we extend our previously established[21,22] two-impurity-level model to study theoretically the crossover instability for the n-GaAs semiconductor under the magnetic field longitudinal to the bias electric field observed in Refs. 1 and 2. The assumption of spatial homogeneity in the x direction, the adoption of the electric field-dependent electron mobility μ_{BH}, and the effects of electron temperature T_e variation, as well as considerations of the magnetic

effects through the Landau level shifts for the electrons in the conduction band, the magnetoresistance property, and the modification on the cross sections of the impact ionization are all retained in this work. In addition, since we are examining the semiconductor with the planar ohmic contacts, a simple relaxation-type equation is introduced phenomenologically[24] for the effective magnetoresistance h factor from the generation-annihilation dynamic of the filamentary current. Studies for the case of the point contact geometry allowing a perpendicular magnetic field can be found in a recent work[38] (and references therein) with the two-level model using totally spatial inhomogeneous time dependent simulation filament current without the h factor. Furthermore, because around the post-breakdown region, the visible variations of the electron temperature T_e, the impact ionization coefficient from the impurity ground level X_1, and the capture coefficient T_1^s with the electric field E (Refs. 23 and 25) suggest the non-negligible T_e dependence in each of these GR coefficients, we add in proper modifications to fulfill this implication. The above phenomenological dynamics for the effective magnetoresistance h factor and the T_e dependence in the GR processes are indeed two important constituents for our model's satisfactory description of the system's bifurcation to chaos via various period-doubling routes.

Having finished the main structure of our theoretical model, we are ready to proceed with numerical simulations. Choosing a magnetic field B above a critical B_c beyond the region after the disappearance of the hysteresis, we solve the differential equations that include the dynamic variables ν, ν_{t_1}, E, h, $\bar{T}_e$ by raising the bias field E_0. We can see the system undergo various oscillations in the ν-E plane and above a certain magnitude of B we can eventually see chaos take place. Our numerical results exhibit the main features of the experimental observations in Refs. 1 and 2.

Together with our previous works,[21,22] we are able to describe the experimental observed phenomena of the hysteresis and the current instability for the n-GaAs semiconductor under an external magnetic field[1,2,19] in the two-impurity-level model consistently. Of course, as we stated in our previous work,[21] since it is a macroscopic model, we do not expect that it can interpret all microscopic properties of the system and some refinements from microscopic aspects may be needed to make the model more complete and perfect. These will be considered in our future work.

ACKNOWLEDGMENTS

We wish to thank Dr. Wei-Feng Hsu and Dr. How-foo Chen for valuable discussions.

*Electronic address: sytsay@ntut.edu.tw

[1] K. Aoki, Y. Kawase, K. Yamamoto, and N. Mugibayashi, J. Phys. Soc. Jpn. **59**, 20 (1990).
[2] K. Aoki, T. Kondo, and T. Watanabe, Solid State Commun. **77**, 91 (1991).
[3] E. Schöll, *Nonequilibrium Phase Transitions in Semiconductors* (Springer, Berlin, 1987).
[4] E. Schöll and D. Drasdo, Z. Phys. B: Condens. Matter **81**, 183 (1990).
[5] A. Brandl and W. Prettl, Phys. Rev. Lett. **66**, 3044 (1991).
[6] G. Hüpper, K. Pyragas, and E. Schöll, Phys. Rev. B **47**, 15515 (1993).
[7] V. Novák, C. Wimmer, and W. Prettl, Phys. Rev. B **52**, 9023 (1995).
[8] E. Kunz and E. Schöll, Z. Phys. B: Condens. Matter **89**, 289 (1992).
[9] E. Schöll, Solid-State Electron. **32**, 1129 (1989).
[10] K. Kardell, C. Radehaus, R. Dohmen, and H.-G. Purwins, J. Appl. Phys. **64**, 6336 (1988).
[11] F. S. Lee and Y. C. Cheng, Chin. J. Phys. (Taipei) **38**, 155 (2000).
[12] R. Obermaier, W. Böhm, W. Prettl, and P. Dirnhofer, Phys. Lett. **105A**, 149 (1984).
[13] E. Schöll, Physica B & C **134**, 271 (1985).
[14] E. Schöll, J. Parisi, B. Röhricht, J. Peinke, and R. P. Huebener, Phys. Lett. A **119**, 419 (1987).
[15] M. Weispfenning, I. Hoeser, W. Böhm, W. Prettl, and E. Schöll, Phys. Rev. Lett. **55**, 754 (1985).
[16] K. Aoki, T. Kobayashi, and K. Yamamoto, J. Phys. Soc. Jpn. **51**, 2373 (1982).
[17] K. Aoki and K. Yamamoto, Phys. Lett. **98A**, 72 (1983).
[18] G. Hüpper, E. Schöll, and A. Rein, Mod. Phys. Lett. B **6**, 1001 (1992).
[19] J. Spangler, A. Brandl, and W. Prettl, Appl. Phys. A: Solids Surf. **48**, 143 (1989).
[20] K. Aoki and T. Kondo, Phys. Lett. A **154**, 281 (1991).
[21] Shwu-Yun Tsay Tzeng and Y. Tzeng, Phys. Rev. B **70**, 085208 (2004).
[22] Shwu-Yun Tsay Tzeng and Y. C. Cheng, Phys. Rev. B **68**, 035211 (2003).
[23] M. Gaa, R. E. Kunz, and E. Schöll, Phys. Rev. B **53**, 15971 (1996).
[24] K. Aoki, Phys. Lett. A **152**, 485 (1991).
[25] B. Kehrer, W. Quade, and E. Schöll, Phys. Rev. B **51**, 7725 (1995).
[26] K. Aoki, Solid State Commun. **77**, 87 (1991).
[27] J. Spangler, U. Margull, and W. Prettl, Phys. Rev. B **45**, R12137 (1992).
[28] K. Aoki, *Nonlinear Dynamics and Chaos in Semiconductors* (IOP, Bristol, 2000).
[29] V. Novák, J. Hirschinger, F.-J. Niedernostheide, W. Prettl, M. Cukr, and J. Oswald, Phys. Rev. B **58**, 13099 (1998).
[30] M. Gaa, R. E. Kunz, E. Schöll, W. Eberle, J. Hirschinger, and W. Prettl, Semicond. Sci. Technol. **11**, 1646 (1996).
[31] K. Aoki, U. Rau, J. Peinke, J. Parisi, and R. P. Huebener, J. Phys. Soc. Jpn. **59**, 420 (1990).
[32] U. Rau, K. Aoki, J. Peinke, J. Parisi, W. Clauss, and R. P. Huebener, Z. Phys. B: Condens. Matter **81**, 53 (1990).
[33] G. Schwarz, C. Lehmann, A. Reimann, E. Schöll, J. Hirschinger, W. Prettl, and V. Novák, Semicond. Sci. Technol. **15**, 593 (2000).

[34] F.-J. Niedernostheide, J. Hirschinger, W. Prettl, V. Novák, and H. Kostial, Phys. Rev. B **58**, 4454 (1998).
[35] K. Seeger, *Semiconductor Physics, An Introduction* (Springer, Berlin, 1999).
[36] W. Shockley, Solid-State Electron. **2**, 35 (1961).
[37] R. M. Westervelt and S. W. Teltsworth, J. Appl. Phys. **57**, 5457 (1985).
[38] J. Murawski, G. Schwarz, V. Novak, W. Prettl, and E. Schöll, Z. Angew. Math. Mech. **85**, 823 (2005).